ACS Energy LETTERS

http://pubs.acs.org/journal/aelccp

LETTER

PbSe Quantum Dot Solar Cells Based on Directly Synthesized Semiconductive Inks

Yang Liu,[⊥] Fei Li,[⊥] Guozheng Shi, Zeke Liu,* Xiaofang Lin, Yao Shi, Yifan Chen, Xing Meng, You Lv, Wei Deng, Xiangqiang Pan,* and Wanli Ma*

Cite This: *ACS Energy Lett.* 2020, 5, 3797−3803

Read Online

ACCESS | Metrics & More | Article Recommendations | Supporting Information

ABSTRACT: The unstable PbSe quantum dot (QD) surface requires tedious and complicated synthetic protocols and renders them substantially underdeveloped compared to PbS QDs. Here, we describe a direct synthesis of PbSe QD inks at room temperature. In comparison to the conventional three-step synthesis, our strategy simplifies the fabrication process to one step and reduces the preparation cost by a factor of eight. A photovoltaic device based on these PbSe QD inks has achieved a photovoltaic conversion efficiency (PCE) of 10.38% with high device stability, which is one of the highest PCEs for all reported PbSe QD solar cells. More importantly, the obtained ink has demonstrated the best colloidal stability by far compared with all the reported lead chalcogenides (PbX) QD inks for photovoltaic application. This simple and low-cost synthesis will facilitate ink storage and transport and may ignite a new round of research efforts on the optoelectronic applications of PbSe QDs.

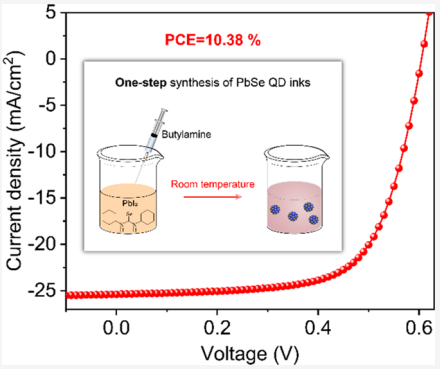

PbSe nanocrystals or quantum dots (QDs) are strongly quantum confined materials with a huge exciton Bohr radius of 46 nm.[1−7] Their absorption can be easily tuned to cover the spectrum from ∼600 nm up to 4000 nm,[2,6] endowing PbSe QDs with the feasibility for use in solution-processable optoelectronic applications, including solar cells,[6,8−16] photodetectors,[17,18] and field-effect transistors.[19−24] Benefiting from their strong quantum confinement, the close-packed PbSe QD solid possess high interdot exciton coupling energy, which is comparable to their exciton binding energy (∼100 meV).[25] This allows significant elongation of the electronic wave function out of QDs, leading to efficient exciton dissociation at room temperature and high carrier mobility without sintering. Therefore, PbSe QDs are ideal building blocks to construct low-cost and printable solar cells. Meanwhile, the remarkable confinement of PbSe QDs gives rise to the multiple exciton generation (MEG) effect, which can push the theoretical photovoltaic efficiency over the S−Q limit. In addition, a peak external quantum efficiency (EQE) of 114% has already been demonstrated via MEG in a functional PbSe QD solar cell.[26,27]

Although PbSe QDs possess larger Bohr radius and greater charge mobility and bandgap tunability than PbS QDs,[4,5,28] the solar cells based on PbSe QDs have been far less explored compared to the widely investigated PbS QDs solar cells. The main issue of PbSe QDs is their susceptibility toward oxygen because of the vulnerable Se on the under-coordinated (100) facets. Several postsynthetic treatments have been invented to improve the air stability of PbSe QDs in solution,[29−31] among which the cation exchange method shows the best performance in photovoltaic application.[8,32,33] To date, PbSe QD solar cells with photovoltaic conversion efficiency (PCE) > 6% have all employed this strategy (Table S1), which consists of three steps: (1) synthesis of CdSe or ZnSe QDs, (2) subsequent cation exchange with lead salt to acquire PbSe QDs, and (3) ligand exchange to prepare semiconductive QD inks for device fabrication (Figure 1a). The preparation processes of PbSe QD inks are apparently more tedious compared to those of PbS QD inks. Furthermore, the estimated material costs for the PbSe QD inks reach 95.0 $\$\cdot g^{-1}$ (Table S2), which is much greater than the preparation cost of PbS QD inks (16.9−35.3 $\$\cdot g^{-1}$).[34] As a result, the complex manufacturing and high cost have certainly impeded the development of PbSe QD solar cells.

Inspired by our recent report on the direct synthesis of PbS QD inks,[35] we further developed a "one-step" method to directly synthesize semiconductive PbSe QD inks. The reaction is conducted by using lead halide and rationally designed selenourea derivatives as precursors under room

Received: September 20, 2020
Accepted: November 9, 2020
Published: November 13, 2020

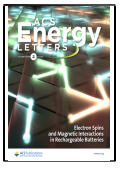

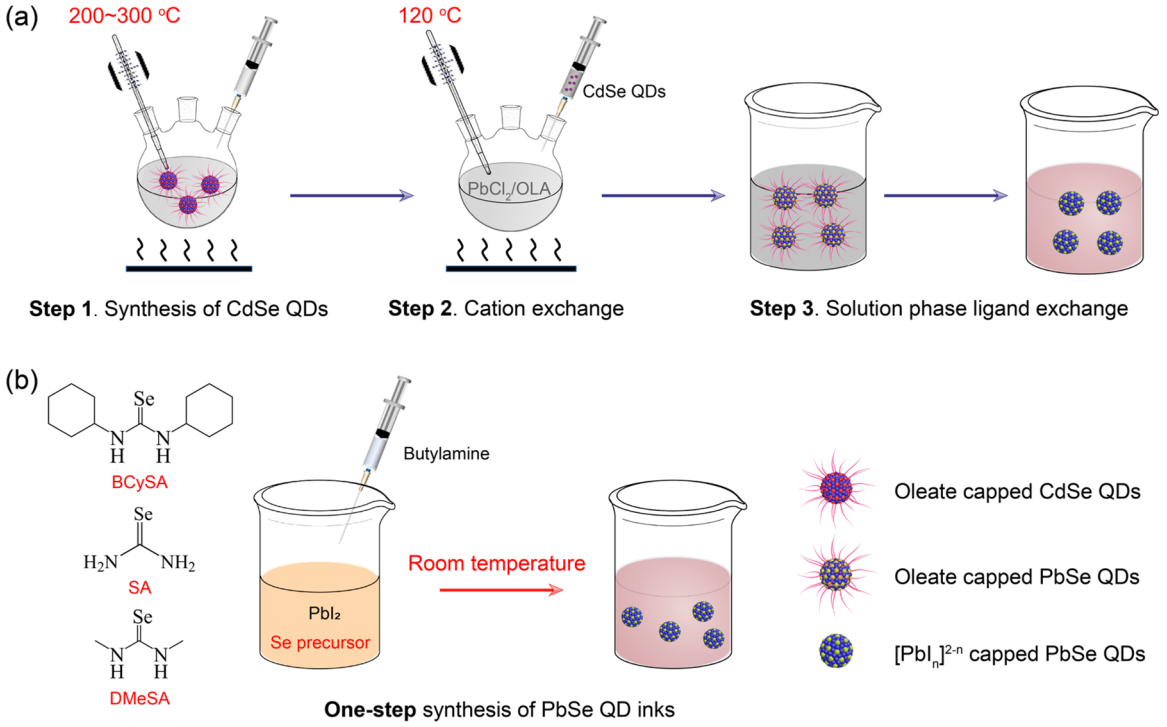

Figure 1. Schematic representation of different synthesis methods for PbSe QD inks. (a) Conventional "three-step" synthesis process, including synthesis of CdSe QDs, cation exchange, and ligand exchange. (b) "One-step", direct synthesis of lead iodide complexes ($[PbI_n]^{2-n}$) capped PbSe QD inks.

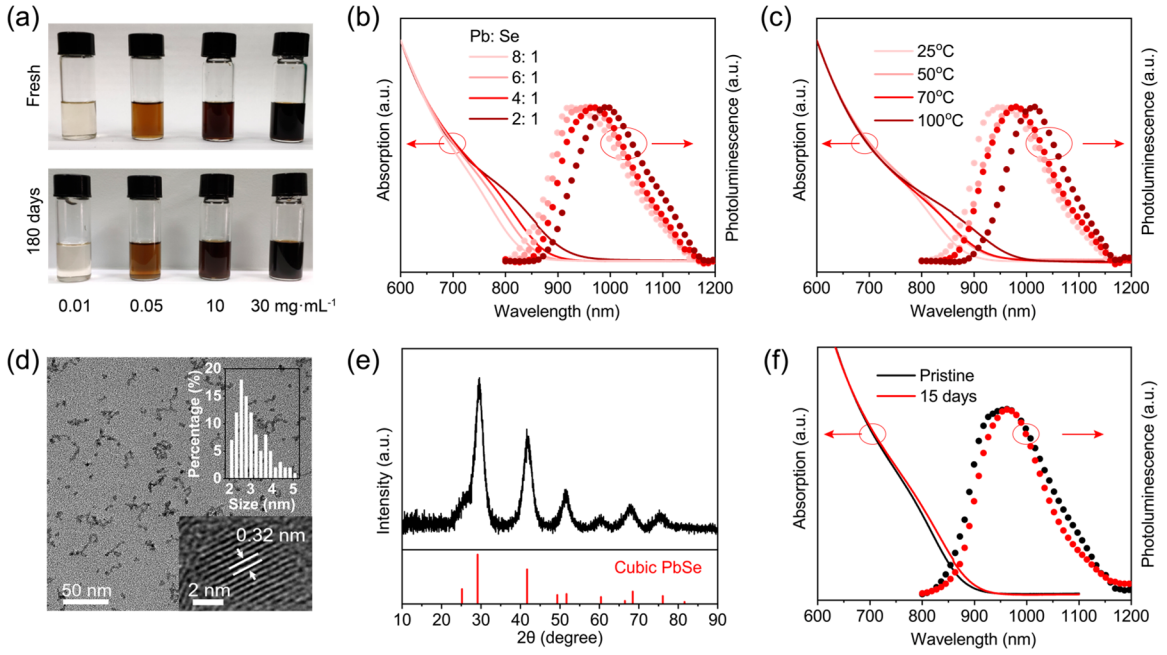

Figure 2. (a) Colloidal stability of PbSe QD inks with different concentrations. Absorption and photoluminescence spectra of PbSe QDs synthesized with (b) different Pb/Se precursor ratios and (c) temperatures. The reaction temperature is 25 °C in panel b. The Pb/Se precursor ratio is 6:1 in panel c. (d) TEM images and (e) XRD pattern of PbSe QDs synthesized with Pb/Se precursor ratio of 6:1 under 25 °C. (f) Absorption and photoluminescence spectra of pristine and aged PbSe QDs.

temperature. The photovoltaic devices based on these directly synthesized PbSe inks show a PCE up to 10.38%, which is one of the highest PCEs for all reported PbSe QD solar cells. It is worth nothing that the *in situ* passivation by the lead halide complexes ($[PbI_n]^{2-n}$) endows the obtained PbSe QD inks with excellent air and colloidal stability. No ink aggregations were observed for at least half a year with a concentration from 0.01 to 30 mg·mL^{-1}, while most reported PbX ink could not survive a day. More importantly, the PCE for the device using aged ink (ink stored under ambient air for 15 days) can reach 90% of the PCE value for a device using the fresh ink, which has demonstrated the best ink colloidal stability for photo-

https://dx.doi.org/10.1021/acsenergylett.0c02011
ACS Energy Lett. 2020, 5, 3797−3803

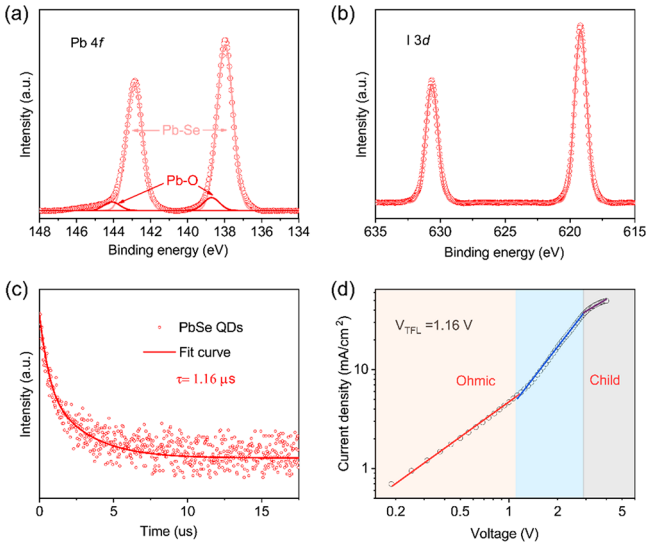

Figure 3. (a) Pb 4f XPS spectrum and (b) I 3d XPS spectrum of PbSe QDs. (c) Transient photoluminescence of PbSe QDs solution. (d) *J*–*V* curve of space charge limited current (SCLC) device of PbSe QD film. Device structure: ITO/ZnO/PbSe QDs/LiF/Ag.

voltaic application compared to all the previous reports, providing a large potential for the operability of ink transport and storage during mass manufacture.

The synthesis of PbSe QD inks is conducted as depicted in Figure 1b. Selenourea (SA), *N*,*N*-dimethyl selenourea (DMeSA), and *N*,*N*-bicyclohexane selenourea (BCySA) compounds with designed reactivity were rationally chosen as Se precursors (with the molecular formulas shown in Figure 1b). The detailed synthesis and characterization of the organic Se precursors are shown in the Supporting Information and Figure S1. The lead iodide (PbI_2) and selenourea derivatives are first dissolved in dimethylformamide (DMF) under nitrogen conditions. Butyl amine (BA) was then swiftly injected into the solution to trigger the reaction. The solution color turned from yellow to black immediately. We conclude that the reaction mechanism can be analogous to that in the direct synthesis of PbS QD inks.[35] BA can interact with selenoureas derivatives to release highly reactive HSe^-, which can react with PbI_2 to rapidly produce PbSe QDs. However, BA should be injected into the mixture of PbI_2 and selenoureas derivatives in less than a few minutes after their dissolution. Otherwise, PbI_2 will react with the selenium precursor, forming black precipitates even in the absence of BA. This is notably different from previous observation in the direct synthesis of PbS QD inks, in which PbI_2 cannot react directly with thiourea without BA.[35] This can be attributed to the reaction activity of selenourea being higher than that of the thiourea.[5] The obtained PbSe QDs can be purified by adding toluene as antisolvent and then redispersed in DMF with an adjustable concentration from ~100 to 1000 mg·mL^{-1}, after which the ink can be used directly for device preparation. Interestingly, the ink can be diluted to as low as 0.01 mg·mL^{-1} with acetonitrile (ACN), while the popular PbS QDs ink obtained by solution-phase ligand-exchange cannot retain colloidal stability with such dilution. In addition, these colloidal solutions can be kept stable for at least half a year without noticeable aggregation or precipitation (Figure 2a). The excellent colloidal dispersibility and stability are critical for future mass manufacturing and applications.

The size of PbSe QDs can be controlled by adjusting the ratio of Pb/Se precursor or reaction temperature. As shown in Figure 2b,c, monotonic redshifts of both absorption and photoluminescence (PL) spectra (indicating increased QDs size) are observed with reduced Pb/Se precursor ratio or increased reaction temperature, which follows the same law in the conventional hot-injection reaction.[36] Transmission electron microscopy (TEM) images (Figure 2d) reveal that the average size of the PbSe QDs synthesized with a Pb/Se ratio of 6 at room temperature is 3.0 ± 0.7 nm (BCySA as the Se precursor). The inserted high-resolution TEM (HRTEM) exhibits the single-crystalline nature of the obtained PbSe QDs. Clear lattice fringes with a measured interplanar spacing of about 0.32 nm can be indexed as (111) planes of the rocksalt PbSe phase (Figure 2d). The powder X-ray diffraction (XRD) pattern of the obtained PbSe QD inks also matches well with the bulk PbSe cubic phase structure without any impurity phases (Figure 2e). Even the three selenoureas can all produce phase-pure PbSe QDs (Figure S2), the obtained QDs show different size distributions. As shown in Figure S3, the PL full-width at half-maximum (fwhm) of the PbSe QDs synthesized with different Se precursors follows the trend BCySA < SA < DMeSA. The size distribution of the QDs should also follow the same trend, which can be attributed to the different reactivity of the Se precursors. According to the previous report, the conversion reactivity of selenoureas depends on the number of substituents and their steric properties. The rate increases as the number of substituents decreases, and increasing the steric bulkiness of the substituent groups can increase reactivity under the same number of substituents.[5,37,38] Therefore, the conversion reactivity of selenoureas follows the trend BCySA > SA > DMeSA, which also corresponds to the solution color change speed after injection of the selenoureas. These facts imply that BCySA with the highest reactivity may trigger the nucleation more homogeneously. This is analogous to numerous cases of QD synthesis, where the precursors with high reactivity were normally used to acquire monodispersed QDs.[6,37,39,40] The PbSe QD inks synthesized with BCySA were then used for characterization and device fabrication. Note that the material cost for our "one-step" synthesized PbSe ink is estimated to be 39.5 \$·g^{-1} if using commercial SA as the precursor (Table S3). The cost can be greatly reduced to 12.0 \$·g^{-1} by using home-synthesized BCySA (Table S4), which is about eight times lower than the cost of ink (95.0 \$·g^{-1}) obtained by conventional "three-step" method (Table S2). We believe the cost can be further reduced by optimizing the synthesis protocol of the selenoureas.[5] In short, different Se precursors were used to effectively tune the QD size distribution and achieved significant reduction of materials cost.

For the conventional PbSe QDs, the vulnerable surface can be oxidized quickly to PbO in air in a few days or even several hours, which results in the blue-shift of both absorption and PL spectra because of the decrease of PbSe core size.[29,41] As shown in Figure 2f, the absorption edge of the directly synthesized PbSe QD inks shows no blue-shift after ink storage in air for 15 days. Instead, both absorption and PL spectra show an interesting red-shift, and the PL fwhm decreases simultaneously. To confirm the size change, we then monitored the QDs through dynamic light scattering (DLS). As shown in Figure S4, the size of the PbSe QDs increases

https://dx.doi.org/10.1021/acsenergylett.0c02011
ACS Energy Lett. 2020, 5, 3797−3803

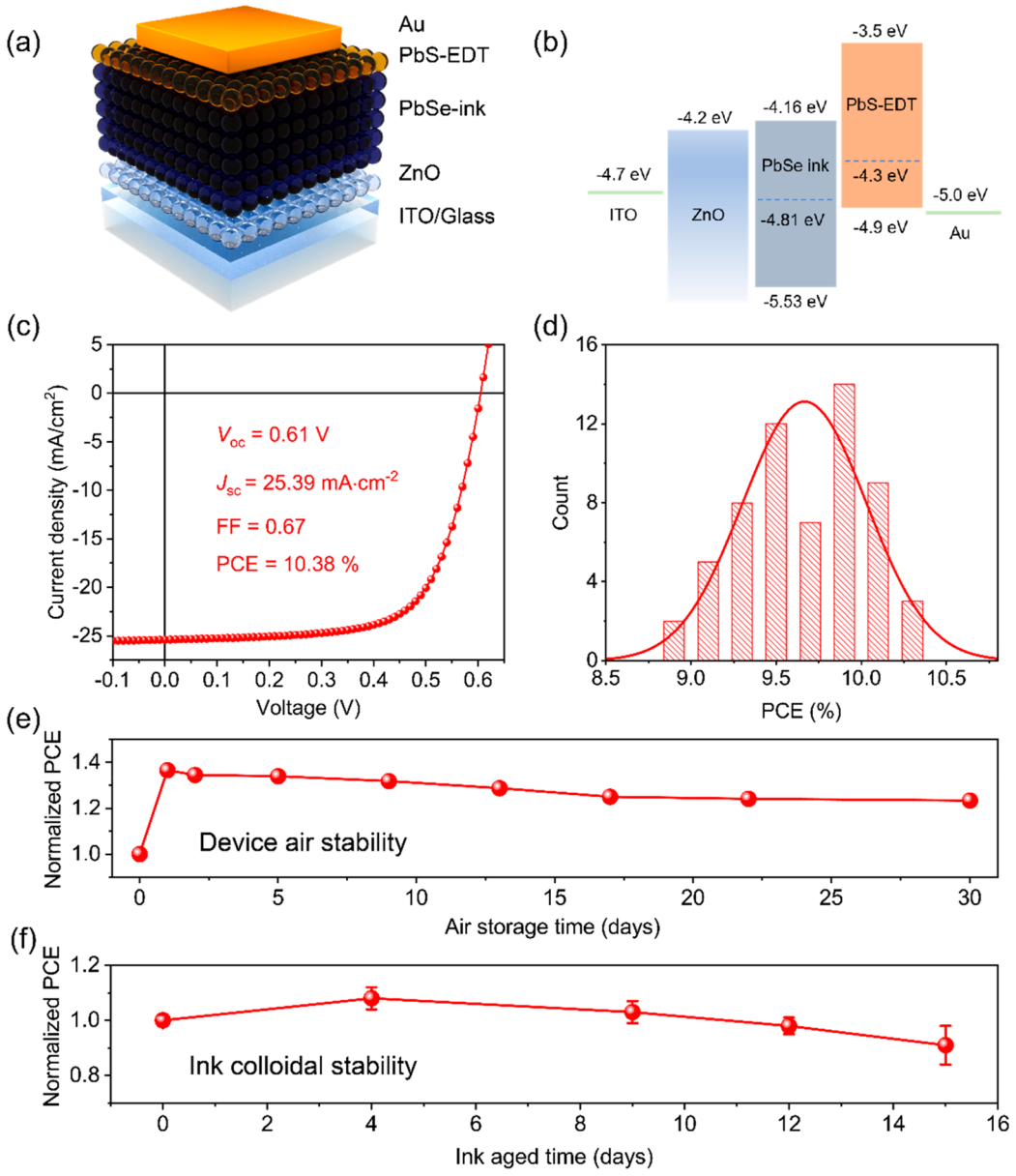

Figure 4. (a) Scheme of the device architecture. (b) Energy level alignment of the solar cell device. (c) *J*–*V* curve of optimized PbSe QD device. (d) Histogram of device efficiency based on 50 devices. (e) Device air stability of PbSe QD-based photovoltaic device. (f) PCE of devices using aged PbSe QD inks with different aging time. The data was normalized by the PCE on the first day in panels e and f.

during storage. These results indicate the isolated PbSe QDs undergo a slow growth and beneficial self-focusing process in the solution because of the little amount of remaining precursors, resulting in spectra red-shift and decreased fwhm, which has also been observed in the PbS QDs previously.[39] In short, no spectra blue-shifts are observed, suggesting the PbSe QDs are substantially more stable in air than those obtained by hot-injection synthesis,[33] which may be attributed to the solid *in situ* passivation with lead iodide complexes.

To ascertain the surface chemistry of the PbSe QDs, we conducted X-ray photoelectron spectroscopy (XPS) measurement. Note that because of very limited reported data for PbSe QD inks, we conducted the comparison mostly between our PbSe QDs and reported PbS QDs. The ratio of iodide to lead (I/Pb) calculated from XPS is 0.89 for directly synthesized PbSe QD inks (Figure 3a,b), which is slightly greater than that of the directly synthesized PbS QD inks (0.84),[35] indicating a greater surface passivants coverage and thus better oxygen protection. As shown in Figure 3c, the time-resolved PL (TRPL) measurement of the PbSe QD inks in DMF exhibits an average decay time of 1.16 μs (Table S5), which is on the same level as that of the directly synthesized PbS QD inks (1.90 μs).[35] To quantify the trap states of PbSe QDs, we have carried out the space charge limited current (SCLC) measurement. As shown in Figure 3d, the calculated trap states density is 3.1×10^{16} cm^{-3}, which is close to the reported values of PbS QD inks.[35,42] The charge transport properties of the PbSe QD film were evaluated by a field-effect transistor (FET) using a bottom-gate top-contact device configuration (Figure S5). The carrier mobility is calculated from the slope of the I_{DS} versus V_{GS} plot in the linear regime according to

$$\mu = \frac{L}{WV_{DS}C_i} \times \frac{\partial I_{DS}}{\partial V_{GS}}$$

https://dx.doi.org/10.1021/acsenergylett.0c02011
ACS Energy Lett. 2020, 5, 3797−3803

where μ is the carrier mobility in the linear regime, I_{DS} the drain current, and V_{GS} the gate voltage; L and W are the channel length (25 μm) and channel width (15 mm), respectively. C_i (11.05 nF/cm^2) is the gate capacitance per unit area, and the C_i was calculated from $C_i = \frac{\varepsilon S}{4\pi k d}$. The calculated μ is 0.0544 cm^2·V^{-1}·s^{-1}, which is greater than the value (0.0267 cm^2·V^{-1}·s^{-1}) obtained from the directly synthesized PbS QD ink film,[35] confirming the superior carrier transport properties of PbSe materials.

The directly synthesized PbSe QD inks were then applied as active layer for the solar cell fabrication. The device structure (ITO/ZnO/PbSe/PbS-EDT (1,2-ethanedithiol)/Au) is shown in Figure 4a, where ZnO and PbS-EDT function as the electron and hole transport layer, respectively.[8,43,44] The energy levels of PbSe QDs were measured by using ultraviolet photoelectron spectroscopy (UPS) (Figure S6), which show appropriate alignments with those of ZnO and PbS-EDT layers (Figure 4b).[45,46] A cross-sectional scanning electron microscopy (SEM) image is shown in Figure S7. The PbSe QD layer can be simply spin-coated from the PbSe QD inks in a single step. The PbSe QD inks synthesized with different Pb/Se precursor ratios were systematically investigated. It is shown that the Pb/Se ratio of 6 gave the best device performance (Figure S8a). The champion device exhibits an open-circuit voltage (V_{oc}) of 0.61 V, a short-circuit current density (J_{sc}) of 25.39 mA·cm^{-2}, and a fill factor (FF) of 0.67, leading to a PCE of 10.38% (Figure 4c), which is one of the highest PCEs for all reported PbSe QD solar cells (Table S1). The J_{sc} is relatively lower than the values reported in the state-of-the-art PbSe QD solar cells,[8,11] which can be attributed to their smaller size in the direct synthesis protocol. The histogram of the device performance characteristics shows decent reproducibility with an average PCE of 9.36% (Figure 4d). The external quantum efficiency (EQE) of the optimized device is shown in Figure S9, and the corresponding integrated J_{sc} values are 24.01 mA·cm^{-2}, which is about 5% error compared to the J_{sc} obtained from the $J-V$ curve. We also fabricated the device using the QD inks synthesized with the other two selenourea precursors; the device performance is slightly lower than that synthesized with BCySA, which may be due to their unsatisfactory size distribution (Figure S8b). Furthermore, the devices can retain around 90% of their initial PCE, after device storage under ambient atmosphere for 30 days, demonstrating excellent device air stability (Figure 4e), which further confirmed the superior surface passivation of the directly synthesized PbSe QD inks. Finally, we sought to investigate how the colloidal stability of the PbSe QD inks affects the photovoltaic performance of solar cells. Figure 4f shows the PCEs of devices using aged PbSe QD inks with different aging times. The device using aged ink with an aging time of 15 days can reach 90% of the PCE value for a device using the fresh ink. The remarkable colloidal stability of our PbSe ink is at the best level for all reported PbX QD inks for photovoltaic application.[46,47] We believe this excellent colloidal stability can support ink transport and storage convenience in real applications. However, we must mention that the current performance of PbSe QD solar cells still lags behind the state-of-the-art PbS cells.[48,49] Future work will focus on the surface chemistry to achieve improved passivation on the vulnerable PbSe QD surface. In addition, further optimization of this new synthesis method to realize better size and homogeneity control may also further improve device performance.

In summary, we have directly synthesized PbSe QD inks in one step at room temperature, successfully avoiding the energy-consuming (200~300 °C) synthesis of CdSe or ZnSe QDs and the tedious cation exchange process in the conventional PbSe QDs synthesis protocol. Moreover, the cost for the preparation of PbSe inks can be reduced approximately eight-fold in comparison to the conventional method. The obtained PbSe QD inks are well passivated and show excellent air stability. Furthermore, the ink has demonstrated the best colloidal stability compared with all the reported PbX QD inks for photovoltaic application. Finally, a PCE of 10.38% based on these PbSe QD inks was achieved with excellent device stability, which is among the highest PCE for all reported PbSe QD solar cells. We believe this simple synthesis method will further unleash the potential of PbSe QDs and promote the development of QD-based optoelectronic applications.

■ ASSOCIATED CONTENT

Supporting Information

The Supporting Information is available free of charge at https://pubs.acs.org/doi/10.1021/acsenergylett.0c02011.

Detailed chemical lists; synthesis of PbSe CQDs and ZnO nanoparticles; device fabrication; synthesis cost estimation; ^{1}H NMR, XRD, UV−vis, PL, DLS, FET, UPS, SEM, and EQE characterizations (PDF)

■ AUTHOR INFORMATION

Corresponding Authors

Zeke Liu − *Institute of Functional Nano & Soft Materials (FUNSOM), Jiangsu Key Laboratory for Carbon-Based Functional Materials & Devices, Joint International Research Laboratory of Carbon-Based Functional Materials and Devices, Soochow University, Suzhou, Jiangsu 215123, P.R. China; State Key Laboratory of Applied Optics, Changchun Institute of Optics, Fine Mechanics and Physics, Chinese Academy of Sciences, Changchun 130033, China;* orcid.org/0000-0002-2507-4386; Email: zkliu@suda.edu.cn

Xiangqiang Pan − *Jiangsu Key Laboratory of Advanced Functional Polymer Design and Application, College of Chemistry, Chemical Engineering and Materials Science, Soochow University, Suzhou 215123, China;* orcid.org/0000-0003-4865-9763; Email: panxq@suda.edu.cn

Wanli Ma − *Institute of Functional Nano & Soft Materials (FUNSOM), Jiangsu Key Laboratory for Carbon-Based Functional Materials & Devices, Joint International Research Laboratory of Carbon-Based Functional Materials and Devices, Soochow University, Suzhou, Jiangsu 215123, P.R. China;* orcid.org/0000-0002-2001-3234; Email: wlma@suda.edu.cn

Authors

Yang Liu − *Institute of Functional Nano & Soft Materials (FUNSOM), Jiangsu Key Laboratory for Carbon-Based Functional Materials & Devices, Joint International Research Laboratory of Carbon-Based Functional Materials and Devices, Soochow University, Suzhou, Jiangsu 215123, P.R. China*

Fei Li − *Institute of Functional Nano & Soft Materials (FUNSOM), Jiangsu Key Laboratory for Carbon-Based Functional Materials & Devices, Joint International Research*

https://dx.doi.org/10.1021/acsenergylett.0c02011
ACS Energy Lett. 2020, 5, 3797−3803

Laboratory of Carbon-Based Functional Materials and Devices, Soochow University, Suzhou, Jiangsu 215123, P.R. China

Guozheng Shi − *Institute of Functional Nano & Soft Materials (FUNSOM), Jiangsu Key Laboratory for Carbon-Based Functional Materials & Devices, Joint International Research Laboratory of Carbon-Based Functional Materials and Devices, Soochow University, Suzhou, Jiangsu 215123, P.R. China*

Xiaofang Lin − *Jiangsu Key Laboratory of Advanced Functional Polymer Design and Application, College of Chemistry, Chemical Engineering and Materials Science, Soochow University, Suzhou 215123, China*

Yao Shi − *Institute of Functional Nano & Soft Materials (FUNSOM), Jiangsu Key Laboratory for Carbon-Based Functional Materials & Devices, Joint International Research Laboratory of Carbon-Based Functional Materials and Devices, Soochow University, Suzhou, Jiangsu 215123, P.R. China*

Yifan Chen − *Institute of Functional Nano & Soft Materials (FUNSOM), Jiangsu Key Laboratory for Carbon-Based Functional Materials & Devices, Joint International Research Laboratory of Carbon-Based Functional Materials and Devices, Soochow University, Suzhou, Jiangsu 215123, P.R. China*

Xing Meng − *Institute of Functional Nano & Soft Materials (FUNSOM), Jiangsu Key Laboratory for Carbon-Based Functional Materials & Devices, Joint International Research Laboratory of Carbon-Based Functional Materials and Devices, Soochow University, Suzhou, Jiangsu 215123, P.R. China*

You Lv − *Institute of Functional Nano & Soft Materials (FUNSOM), Jiangsu Key Laboratory for Carbon-Based Functional Materials & Devices, Joint International Research Laboratory of Carbon-Based Functional Materials and Devices, Soochow University, Suzhou, Jiangsu 215123, P.R. China*

Wei Deng − *Institute of Functional Nano & Soft Materials (FUNSOM), Jiangsu Key Laboratory for Carbon-Based Functional Materials & Devices, Joint International Research Laboratory of Carbon-Based Functional Materials and Devices, Soochow University, Suzhou, Jiangsu 215123, P.R. China;* orcid.org/0000-0002-0067-0624

Complete contact information is available at: https://pubs.acs.org/10.1021/acsenergylett.0c02011

Author Contributions

[⊥]Y.L. and F.L. contributed equally to this work.

Notes

The authors declare no competing financial interest.

■ ACKNOWLEDGMENTS

This work was supported by the National Key Research Projects (Grant No. 2016YFA0202402), the National Natural Science Foundation of China (Grant Nos. 52002260, 51803144, 61674111, and 21971177), and "111" projects. The authors thank the Collaborative Innovation Center of Suzhou Nano Science and Technology, Soochow University, the Priority Academic Program Development of Jiangsu Higher Education Institutions (PAPD). The Project was also Supported by the State Key Laboratory of applied optics (Grant No. SKLAO2020001A03).

■ REFERENCES

(1) Murray, C.; Sun, S.; Gaschler, W.; Doyle, H.; Betley, T.; Kagan, C. Colloidal Synthesis of Nanocrystals and Nanocrystal Superlattices. *IBM J. Res. Dev.* **2001**, *45*, 47.

(2) Pietryga, J. M.; Schaller, R. D.; Werder, D.; Stewart, M. H.; Klimov, V. I.; Hollingsworth, J. A. Pushing the Band Gap Envelope: Mid-Infrared Emitting Colloidal PbSe Quantum Dots. *J. Am. Chem. Soc.* **2004**, *126*, 11752.

(3) Yu, W. W.; Falkner, J. C.; Shih, B. S.; Colvin, V. L. Preparation and Characterization of Monodisperse PbSe Semiconductor Nanocrystals in a Noncoordinating Solvent. *Chem. Mater.* **2004**, *16*, 3318.

(4) Lian, L.; Xia, Y.; Zhang, C.; Xu, B.; Yang, L.; Liu, H.; Zhang, D.; Wang, K.; Gao, J.; Zhang, J. In Situ Tuning the Reactivity of Selenium Precursor to Synthesize Wide Range Size, Ultralarge-Scale, and Ultrastable PbSe Quantum Dots. *Chem. Mater.* **2018**, *30*, 982.

(5) Campos, M. P.; Hendricks, M. P.; Beecher, A. N.; Walravens, W.; Swain, R. A.; Cleveland, G. T.; Hens, Z.; Sfeir, M. Y.; Owen, J. S. A Library of Selenourea Precursors to PbSe Nanocrystals with Size Distributions near the Homogeneous Limit. *J. Am. Chem. Soc.* **2017**, *139*, 2296.

(6) Ma, W.; Swisher, S. L.; Ewers, T.; Engel, J.; Ferry, V. E.; Atwater, H. A.; Alivisatos, A. P. Photovoltaic Performance of Ultrasmall PbSe Quantum Dots. *ACS Nano* **2011**, *5*, 8140.

(7) Wise, F. W. Lead Salt Quantum Dots: The Limit of Strong Quantum Confinement. *Acc. Chem. Res.* **2000**, *33*, 773.

(8) Ahmad, W.; He, J.; Liu, Z.; Xu, K.; Chen, Z.; Yang, X.; Li, D.; Xia, Y.; Zhang, J.; Chen, C. Lead Selenide (PbSe) Colloidal Quantum Dot Solar Cells with > 10% Efficiency. *Adv. Mater.* **2019**, *31*, 1900593.

(9) Zhu, M.; Liu, X.; Liu, S.; Chen, C.; He, J.; Liu, W.; Yang, J.; Gao, L.; Niu, G.; Tang, J.; Zhang, J. Efficient PbSe Colloidal Quantum Dot Solar Cells Using SnO_2 as a Buffer Layer. *ACS Appl. Mater. Interfaces* **2020**, *12*, 2566.

(10) Hu, L.; Zhang, Z.; Patterson, R. J.; Shivarudraiah, S. B.; Zhou, Z.; Ng, M.; Huang, S.; Halpert, J. E. PbSe Quantum Dot Passivated Via Mixed Halide Perovskite Nanocrystals for Solar Cells with over 9% Efficiency. *Solar RRL* **2018**, *2*, 1800234.

(11) Hu, L.; Geng, X.; Singh, S.; Shi, J.; Hu, Y.; Li, S.; Guan, X.; He, T.; Li, X.; Cheng, Z.; Patterson, R.; Huang, S.; Wu, T. Synergistic Effect of Electron Transport Layer and Colloidal Quantum Dot Solid Enable PbSe Quantum Dot Solar Cell Achieving over 10% Efficiency. *Nano Energy* **2019**, *64*, 103922.

(12) Luther, J. M.; Law, M.; Beard, M. C.; Song, Q.; Reese, M. O.; Ellingson, R. J.; Nozik, A. J. Schottky Solar Cells Based on Colloidal Nanocrystal Films. *Nano Lett.* **2008**, *8*, 3488.

(13) Liu, Z.; Yuan, J.; Hawks, S. A.; Shi, G.; Lee, S.-T.; Ma, W. Photovoltaic Devices Based on Colloidal PbX Quantum Dots: Progress and Prospects. *Solar RRL* **2017**, *1*, 1600021.

(14) Carey, G. H.; Abdelhady, A. L.; Ning, Z.; Thon, S. M.; Bakr, O. M.; Sargent, E. H. Colloidal Quantum Dot Solar Cells. *Chem. Rev.* **2015**, *115*, 12732.

(15) Zhang, Y.; Wu, G.; Ding, C.; Liu, F.; Yao, Y.; Zhou, Y.; Wu, C.; Nakazawa, N.; Huang, Q.; Toyoda, T.; Wang, R.; Hayase, S.; Zou, Z.; Shen, Q. Lead Selenide Colloidal Quantum Dot Solar Cells Achieving High Open-Circuit Voltage with One-Step Deposition Strategy. *J. Phys. Chem. Lett.* **2018**, *9*, 3598.

(16) Zhang, Z.; Chen, Z.; Yuan, L.; Chen, W.; Yang, J.; Wang, B.; Wen, X.; Zhang, J.; Hu, L.; Stride, J. A.; Conibeer, G. J.; Patterson, R. J.; Huang, S. A New Passivation Route Leading to over 8% Efficient PbSe Quantum-Dot Solar Cells Via Direct Ion Exchange with Perovskite Nanocrystals. *Adv. Mater.* **2017**, *29*, 1703214.

(17) Zhu, T.; Zheng, L.; Yao, X.; Liu, L.; Huang, F.; Cao, Y.; Gong, X. Ultrasensitive Solution-Processed Broadband PbSe Photodetectors through Photomultiplication Effect. *ACS Appl. Mater. Interfaces* **2019**, *11*, 9205.

(18) Manga, K. K.; Wang, J.; Lin, M.; Zhang, J.; Nesladek, M.; Nalla, V.; Ji, W.; Loh, K. P. High-Performance Broadband Photodetector Using Solution-Processible PbSe-TiO_2-Graphene Hybrids. *Adv. Mater.* **2012**, *24*, 1697.

(19) Sayevich, V.; Gaponik, N.; Plötner, M.; Kruszynska, M.; Gemming, T.; Dzhagan, V. M.; Akhavan, S.; Zahn, D. R. T.; Demir, H. V.; Eychmüller, A. Stable Dispersion of Iodide-Capped PbSe Quantum Dots for High-Performance Low-Temperature Processed Electronics and Optoelectronics. *Chem. Mater.* **2015**, *27*, 4328.
(20) Balazs, D. M.; Matysiak, B. M.; Momand, J.; Shulga, A. G.; Ibanez, M.; Kovalenko, M. V.; Kooi, B. J.; Loi, M. A. Electron Mobility of 24 $cm^2V^{-1}S^{-1}$ in PbSe Colloidal-Quantum-Dot Superlattices. *Adv. Mater.* **2018**, *30*, 1802265.
(21) Han, L.; Balazs, D. M.; Shulga, A. G.; Abdu-Aguye, M.; Ma, W.; Loi, M. A. PbSe Nanorod Field-Effect Transistors: Room- and Low-Temperature Performance. *Adv. Electron. Mater.* **2018**, *4*, 1700580.
(22) Oh, S. J.; Wang, Z.; Berry, N. E.; Choi, J. H.; Zhao, T.; Gaulding, E. A.; Paik, T.; Lai, Y.; Murray, C. B.; Kagan, C. R. Engineering Charge Injection and Charge Transport for High Performance PbSe Nanocrystal Thin Film Devices and Circuits. *Nano Lett.* **2014**, *14*, 6210.
(23) Talapin, D. V.; Murray, C. B. PbSe Nanocrystal Solids for N- and P-Channel Thin Film Field-Effect Transistors. *Science* **2005**, *310*, 86.
(24) Kagan, C. R.; Murray, C. B. Charge Transport in Strongly Coupled Quantum Dot Solids. *Nat. Nanotechnol.* **2015**, *10*, 1013.
(25) Choi, J. J.; Luria, J.; Hyun, B.-R.; Bartnik, A. C.; Sun, L.; Lim, Y.-F.; Marohn, J. A.; Wise, F. W.; Hanrath, T. Photogenerated Exciton Dissociation in Highly Coupled Lead Salt Nanocrystal Assemblies. *Nano Lett.* **2010**, *10*, 1805.
(26) Semonin, O. E.; Luther, J. M.; Choi, S.; Chen, H. Y.; Gao, J.; Nozik, A. J.; Beard, M. C. Peak External Photocurrent Quantum Efficiency Exceeding 100% Via MEG in a Quantum Dot Solar Cell. *Science* **2011**, *334*, 1530.
(27) Beard, M. C.; Luther, J. M.; Semonin, O. E.; Nozik, A. J. Third Generation Photovoltaics Based on Multiple Exciton Generation in Quantum Confined Semiconductors. *Acc. Chem. Res.* **2013**, *46*, 1252.
(28) Midgett, A. G.; Luther, J. M.; Stewart, J. T.; Smith, D. K.; Padilha, L. A.; Klimov, V. I.; Nozik, A. J.; Beard, M. C. Size and Composition Dependent Multiple Exciton Generation Efficiency in PbS, PbSe, and PbS_XSe_{1-X} Alloyed Quantum Dots. *Nano Lett.* **2013**, *13*, 3078.
(29) Woo, J. Y.; Ko, J. H.; Song, J. H.; Kim, K.; Choi, H.; Kim, Y. H.; Lee, D. C.; Jeong, S. Ultrastable PbSe Nanocrystal Quantum Dots Via in Situ Formation of Atomically Thin Halide Adlayers on PbSe(100). *J. Am. Chem. Soc.* **2014**, *136*, 8883.
(30) Bae, W. K.; Joo, J.; Padilha, L. A.; Won, J.; Lee, D. C.; Lin, Q.; Koh, W. K.; Luo, H.; Klimov, V. I.; Pietryga, J. M. Highly Effective Surface Passivation of PbSe Quantum Dots through Reaction with Molecular Chlorine. *J. Am. Chem. Soc.* **2012**, *134*, 20160.
(31) Woo, J. Y.; Lee, S.; Lee, S.; Kim, W. D.; Lee, K.; Kim, K.; An, H. J.; Lee, D. C.; Jeong, S. Air-Stable PbSe Nanocrystals Passivated by Phosphonic Acids. *J. Am. Chem. Soc.* **2016**, *138*, 876.
(32) Kim, S.; Marshall, A. R.; Kroupa, D. M.; Miller, E. M.; Luther, J. M.; Jeong, S.; Beard, M. C. Air-Stable and Efficient PbSe Quantum-Dot Solar Cells Based Upon ZnSe to PbSe Cation-Exchanged Quantum Dots. *ACS Nano* **2015**, *9*, 8157.
(33) Zhang, J.; Gao, J.; Church, C. P.; Miller, E. M.; Luther, J. M.; Klimov, V. I.; Beard, M. C. PbSe Quantum Dot Solar Cells with More Than 6% Efficiency Fabricated in Ambient Atmosphere. *Nano Lett.* **2014**, *14*, 6010.
(34) Jean, J.; Xiao, J.; Nick, R.; Moody, N.; Nasilowski, M.; Bawendi, M.; Bulović, V. Synthesis Cost Dictates the Commercial Viability of Lead Sulfide and Perovskite Quantum Dot Photovoltaics. *Energy Environ. Sci.* **2018**, *11*, 2295.
(35) Wang, Y.; Liu, Z.; Huo, N.; Li, F.; Gu, M.; Ling, X.; Zhang, Y.; Lu, K.; Han, L.; Fang, H.; Shulga, A. G.; Xue, Y.; Zhou, S.; Yang, F.; Tang, X.; Zheng, J.; Antonietta Loi, M.; Konstantatos, G.; Ma, W. Room-Temperature Direct Synthesis of Semi-Conductive PbS Nanocrystal Inks for Optoelectronic Applications. *Nat. Commun.* **2019**, *10*, 5136.
(36) Moreels, I.; Justo, Y.; De Geyter, B.; Haustraete, K.; Martins, J. C.; Hens, Z. Size-Tunable, Bright, and Stable PbS Quantum Dots: A Surface Chemistry Study. *ACS Nano* **2011**, *5*, 2004.
(37) Hamachi, L. S.; Jen-La Plante, I.; Coryell, A. C.; De Roo, J.; Owen, J. S. Kinetic Control over CdS Nanocrystal Nucleation Using a Library of Thiocarbonates, Thiocarbamates, and Thioureas. *Chem. Mater.* **2017**, *29*, 8711.
(38) Hendricks, M. P.; Campos, M. P.; Cleveland, G. T.; Jen-La Plante, I.; Owen, J. S. A Tunable Library of Substituted Thiourea Precursors to Metal Sulfide Nanocrystals. *Science* **2015**, *348*, 1226.
(39) Hines, M. A.; Scholes, G. D. Colloidal PbS Nanocrystals with Size-Tunable near-Infrared Emission: Observation of Post-Synthesis Self-Narrowing of the Particle Size Distribution. *Adv. Mater.* **2003**, *15*, 1844.
(40) Murray, C.; Norris, D.; Bawendi, M. G. Synthesis and Characterization of Nearly Monodisperse CdE (E= Sulfur, Selenium, Tellurium) Semiconductor Nanocrystallites. *J. Am. Chem. Soc.* **1993**, *115*, 8706.
(41) Sykora, M.; Koposov, A. Y.; McGuire, J. A.; Schulze, R. K.; Tretiak, O.; Pietryga, J. M.; Klimov, V. I. Effect of Air Exposure on Surface Properties, Electronic Structure, and Carrier Relaxation in PbSe Nanocrystals. *ACS Nano* **2010**, *4*, 2021.
(42) Sun, B.; Voznyy, O.; Tan, H.; Stadler, P.; Liu, M.; Walters, G.; Proppe, A. H.; Liu, M.; Fan, J.; Zhuang, T.; Li, J.; Wei, M.; Xu, J.; Kim, Y.; Hoogland, S.; Sargent, E. H. Pseudohalide-Exchanged Quantum Dot Solids Achieve Record Quantum Efficiency in Infrared Photovoltaics. *Adv. Mater.* **2017**, *29*, 1700749.
(43) Chuang, C. H.; Brown, P. R.; Bulovic, V.; Bawendi, M. G. Improved Performance and Stability in Quantum Dot Solar Cells through Band Alignment Engineering. *Nat. Mater.* **2014**, *13*, 796.
(44) Lu, K.; Wang, Y.; Liu, Z.; Han, L.; Shi, G.; Fang, H.; Chen, J.; Ye, X.; Chen, S.; Yang, F.; Shulga, A. G.; Wu, T.; Gu, M.; Zhou, S.; Fan, J.; Loi, M. A.; Ma, W. High-Efficiency PbS Quantum-Dot Solar Cells with Greatly Simplified Fabrication Processing Via "Solvent-Curing. *Adv. Mater.* **2018**, *30*, 1707572.
(45) Yang, F.; Xu, Y.; Gu, M.; Zhou, S.; Wang, Y.; Lu, K.; Liu, Z.; Ling, X.; Zhu, Z.; Chen, J.; Wu, Z.; Zhang, Y.; Xue, Y.; Li, F.; Yuan, J.; Ma, W. Synthesis of Cesium-Doped ZnO Nanoparticles as an Electron Extraction Layer for Efficient PbS Colloidal Quantum Dot Solar Cells. *J. Mater. Chem. A* **2018**, *6*, 17688.
(46) Gu, M.; Wang, Y.; Yang, F.; Lu, K.; Xue, Y.; Wu, T.; Fang, H.; Zhou, S.; Zhang, Y.; Ling, X.; Xu, Y.; Li, F.; Yuan, J.; Loi, M. A.; Liu, Z.; Ma, W. Stable PbS Quantum Dot Ink for Efficient Solar Cells by Solution-Phase Ligand Engineering. *J. Mater. Chem. A* **2019**, *7*, 15951.
(47) Jia, D.; Chen, J.; Zheng, S.; Phuyal, D.; Yu, M.; Tian, L.; Liu, J.; Karis, O.; Rensmo, H.; Johansson, E. M. J.; Zhang, X. Highly Stabilized Quantum Dot Ink for Efficient Infrared Light Absorbing Solar Cells. *Adv. Energy Mater.* **2019**, *9*, 1902809.
(48) Choi, M. J.; Garcia de Arquer, F. P.; Proppe, A. H.; Seifitokaldani, A.; Choi, J.; Kim, J.; Baek, S. W.; Liu, M.; Sun, B.; Biondi, M.; Scheffel, B.; Walters, G.; Nam, D. H.; Jo, J. W.; Ouellette, O.; Voznyy, O.; Hoogland, S.; Kelley, S. O.; Jung, Y. S.; Sargent, E. H. Cascade Surface Modification of Colloidal Quantum Dot Inks Enables Efficient Bulk Homojunction Photovoltaics. *Nat. Commun.* **2020**, *11*, 103.
(49) Sun, B.; Johnston, A.; Xu, C.; Wei, M.; Huang, Z.; Jiang, Z.; Zhou, H.; Gao, Y.; Dong, Y.; Ouellette, O.; Zheng, X.; Liu, J.; Choi, M.-J.; Gao, Y.; Baek, S.-W.; Laquai, F.; Bakr, O. M.; Ban, D.; Voznyy, O.; García de Arquer, F. P.; Sargent, E. H. Monolayer Perovskite Bridges Enable Strong Quantum Dot Coupling for Efficient Solar Cells. *Joule* **2020**, *4*, 1542.

https://dx.doi.org/10.1021/acsenergylett.0c02011
ACS Energy Lett. 2020, 5, 3797−3803